Biogeochemistry (2021) 153:135–153
https://doi.org/10.1007/s10533-021-00773-z

$\delta^2H_{n\text{-alkane}}$ and $\delta^{18}O_{sugar}$ biomarker proxies from leaves and topsoils of the Bale Mountains, Ethiopia, and implications for paleoclimate reconstructions

Bruk Lemma · Lucas Bittner · Bruno Glaser · Seifu Kebede · Sileshi Nemomissa · Wolfgang Zech · Michael Zech

Received: 7 October 2020 / Accepted: 20 February 2021 / Published online: 16 March 2021

Abstract The hydrogen isotopic composition of leaf wax–derived *n*-alkane ($\delta^2H_{n\text{-alkane}}$) and oxygen isotopic composition of hemicellulose–derived sugar ($\delta^{18}O_{sugar}$) biomarkers are valuable proxies for paleoclimate reconstructions. Here, we present a calibration study along the Bale Mountains in Ethiopia to evaluate how accurately and precisely the isotopic composition of precipitation is imprinted in these biomarkers. *n*-Alkanes and sugars were extracted from the leaf and topsoil samples and compound–specific $\delta^2H_{n\text{-alkane}}$ and $\delta^{18}O_{sugar}$ values were measured using a gas chromatograph–thermal conversion–isotope ratio mass spectrometer (GC–TC–IRMS). The weighted mean $\delta^2H_{n\text{-alkane}}$ and $\delta^{18}O_{sugar}$ values range from − 186 to − 89‰ and from + 27 to + 46‰, respectively. Degradation and root inputs did not appear to alter the isotopic composition of the biomarkers in the soil samples analyzed. Yet, the $\delta^2H_{n\text{-alkane}}$ values show

Responsible Editor: Myrna Simpson.

Supplementary Information The online version contains supplementary material available at https://doi.org/10.1007/s10533-021-00773-z.

B. Lemma (✉) · B. Glaser · M. Zech
Institute of Agronomy and Nutritional Sciences, Soil Biogeochemistry, Martin Luther University Halle-Wittenberg, Von-Seckendorff-Platz 3, 06120 Halle, Germany
e-mail: bruklemma@gmail.com

B. Glaser
e-mail: bruno.glaser@landw.uni-halle.de

M. Zech
e-mail: michael_zech@gmx.de

B. Lemma
Forest and Rangeland Biodiversity Directorate, Ethiopian Biodiversity Institute, P.O. Box 30726, Addis Ababa, Ethiopia

L. Bittner · M. Zech
Institute of Geography, Technische Universität Dresden, Helmholtzstraße 10, 01062 Dresden, Germany
e-mail: lucas.bittner@tu-dresden.de

S. Kebede
Center for Water Resources Research, School of Agricultural, Earth and Environmental Sciences, University of KwaZulu-Natal, Pietermaritzburg 3021, South Africa
e-mail: seifukebede@yahoo.com

S. Nemomissa
Department of Plant Biology and Biodiversity Management, Addis Ababa University, P.O. Box 3434, Addis Ababa, Ethiopia
e-mail: snemomissa@gmail.com

W. Zech
Institute of Soil Science and Soil Geography, University of Bayreuth, Universitätsstraße 30, 95440 Bayreuth, Germany
e-mail: w.zech@uni-bayreuth.de

a statistically significant species dependence and $\delta^{18}O_{sugar}$ yielded the same species–dependent trends. The reconstructed leaf water of *Erica arborea* and *Erica trimera* is ^{2}H– and ^{18}O–enriched by + 55 ± 5 and + 9 ± 1‰, respectively, compared to precipitation. By contrast, *Festuca abyssinica* reveals the most negative $\delta^{2}H_{n\text{-alkane}}$ and least positive $\delta^{18}O_{sugar}$ values. This can be attributed to "signal–dampening" caused by basal grass leaf growth. The intermediate values for *Alchemilla haumannii* and *Helichrysum splendidum* can be likely explained with plant physiological differences or microclimatic conditions affecting relative humidity (RH) and thus RH–dependent leaf water isotope enrichment. While the actual RH values range from 69 to 82% ($\bar{x}$ = 80 ± 3.4%), the reconstructed RH values based on a recently suggested coupled $\delta^{2}H_{n\text{-alkane}}$ –$\delta^{18}O_{sugar}$ (paleo–) hygrometer approach yielded a mean of 78 ± 21%. Our findings corroborate (i) that vegetation changes, particularly in terms of grass versus non–grassy vegetation, need to be considered in paleoclimate studies based on $\delta^{2}H_{n\text{-alkane}}$ and $\delta^{18}O_{sugar}$ records and (ii) that the coupled $\delta^{2}H_{n\text{-alkane}}$ –$\delta^{18}O_{sugar}$ (paleo–) hygrometer approach holds great potential for deriving additional paleoclimatic information compared to single isotope approaches.

Keywords *n*-Alkane · Hydrogen–2 · Sugar · Oxygen–18 · Evapotranspirative enrichment · Paleo–hygrometer

Introduction

The compound–specific hydrogen isotopic composition of leaf wax–derived *n*-alkanes ($\delta^{2}H_{n\text{-alkane}}$) and oxygen isotopic composition of hemicellulose–derived sugars ($\delta^{18}O_{sugar}$) serve as valuable proxies in (paleo)–climate and –environmental studies (e.g. Zech et al. 2013b, 2014a; Tuthorn et al. 2015; Hepp et al. 2017). The above mentioned biomarkers are preserved for a long period of time (Eglinton and Hamilton 1967; Glaser and Zech 2005; Eglinton and Eglinton 2008) and their application was tested in different paleoclimate archives, such as for instance in lake sediments (Zech et al. 2014b; Hepp et al. 2015), loess–paleosols (Zech et al. 2013b; Buggle and Zech 2015), and tree rings (Gessler et al. 2009). The isotopic composition of $\delta^{2}H_{n\text{-alkane}}$ and $\delta^{18}O_{sugar}$ from terrestrial vascular plants primarily reflects the isotopic composition of precipitation. In turn, the isotopic composition of $\delta^{2}H_{prec}$ and $\delta^{18}O_{prec}$ on the continents is mainly controlled by different site and climatic factors. The most prominent factors determining the spatial and temporal variation of $\delta^{2}H_{prec}$ and $\delta^{18}O_{prec}$ were attributed to 'effects' (Dansgaard 1964; Rozanski et al. 1993). For instance, the 'temperature–effect' describes that at lower/higher temperatures $\delta^{2}H_{prec}$ and $\delta^{18}O_{prec}$ values become more negative/positive particularly at higher latitudes. Particularly in many tropical regions, the 'amount–effect' describes that low/high amounts of precipitation typically coincide with more positive/negative $\delta^{2}H_{prec}$ and $\delta^{18}O_{prec}$ values. And finally, more negative $\delta^{2}H_{prec}$ and $\delta^{18}O_{prec}$ values are usually observed at higher elevation due to the 'altitude–effect'. Recent publications emphasize, however, that other factors than $\delta^{2}H_{prec}$ can exert strong control over $\delta^{2}H_{n\text{-alkane}}$, thus preventing $\delta^{2}H_{prec}$ as well as e.g. paleoaltimetry reconstructions (Zech et al. 2015; Coffinet et al. 2017; Jaeschke et al. 2018).

Some studies reveal the absence of isotope fractionation during decomposition (Zech et al. 2012b) and water uptake by the roots (White et al. 1985; Ehleringer et al. 1991; Feakins and Sessions 2010). Nevertheless, caution must be used when using $\delta^{2}H_{n\text{-alkane}}$ for paleoclimate reconstruction due to the effects of degradation and synthesis of leaf wax–derived *n*-alkanes by microorganisms (Brittingham et al. 2017; Zech et al. 2009, 2012a). Similarly, investigations on halophytic and xerophytic plants show evidence of hydrogen isotope fractionation during water uptake at the root–soil interface (Ellsworth and Williams 2007; Ladd and Sachs 2015). Apart from this, it is well known that leaf water is ^{2}H– and ^{18}O–enriched compared to plant source water due to evapotranspiration. This enrichment is primarily dependent on relative humidity (RH) and can challenge a robust $\delta^{2}H_{prec}$ and $\delta^{18}O_{prec}$ reconstruction (Zech et al. 2015). Moreover, the evaporative enrichment of leaf water affects the $\delta^{2}H_{n\text{-alkane}}$ and $\delta^{18}O_{sugar}$ values of monocot and dicot plants at different magnitudes. This latter effect is called "signal–dampening" and causes grasses to have generally more negative/less positive compound–specific stable hydrogen and oxygen isotope values than broad–leaf plant species (Hepp et al. 2019, 2020a). Hence, the interpretation of the isotopic

composition of plant–derived biomarkers should consider (i) the isotopic composition of precipitation, (ii) RH– dependent evapotranspirative enrichment of leaf water, (iii) biosynthetic fractionation and signal–dampening (cf. section 'Conceptual framework for interpreting the coupled $\delta^2H_{n\text{-alkane}}$–$\delta^{18}O_{sugar}$ approach: reconstruction of leaf water, source water, *d*-excess, and relative humidity').

Some years ago, Zech et al. (2013b) proposed a coupled $\delta^2H_{n\text{-alkane}}$ –$\delta^{18}O_{sugar}$ approach. This coupled approach aims at providing additional information to reconstruct paleoclimate and allows the reconstruction of δ^2H and $\delta^{18}O$ source water ($\delta^2H_{source\ water}$ and $\delta^{18}O_{source\ water}$) and deuterium excess (*d*-excess, a proxy for RH). This approach was validated using climate transects across Argentina (Tuthorn et al. 2015) and South Africa (Strobel et al. 2020) as well as using a climate chamber experiment (Hepp et al. 2020b) and yielded highly significant correlations between actual and reconstructed RH and precipitation. The coupled approach was also successfully applied to eolian/loess–paleosol sediments and lacustrine sediments to reconstruct paleoclimate changes (Zech et al. 2013b; Hepp et al. 2017, 2019). The concept of using both δ^2H and $\delta^{18}O$ was independently developed for tree–ring cellulose to deduce RH (Voelker et al. 2014).

The main objective of the present study was to evaluate how accurately and precisely the isotopic signature of contemporary precipitation and RH are imprinted on compound–specific stable isotopes of leaves and topsoils of the Bale Mountains. More specifically, we aim at answering the following questions: (I) Are there systematic $\delta^2H_{n\text{-}\ alkane}$ and $\delta^{18}O_{sugar}$ differences between leaves, O–layers, and A_h–horizons? (II) Do *n*-alkane and sugar biomarkers in leaves and topsoils reflect δ^2H_{prec} and $\delta^{18}O_{prec}$? (III) Are there systematic $\delta^2H_{n\text{-alkane}}$ and $\delta^{18}O_{sugar}$ differences among the locally dominant plant species? (IV) Does the application of the coupled $\delta^2H_{n\text{-alkane}}$ – $\delta^{18}O_{sugar}$ (paleo–) hygrometer approach provide additional information compared to the single isotope approaches?

Material and methods

Geography of the Bale Mountains

The Bale Mountains are located 400 km southeast of Addis Ababa, capital of Ethiopia, and belong to the Bale–Arsi Mountains massif (Fig. 1). The Bale Mountains National Park (BMNP) is situated between 39° 28′ to 39° 57′ longitude (E) and between 6° 29′ to 7° 10′ latitude (N), spanning a large altitudinal (1400–4377 m a.s.l.) gradient (Hillman 1986, 1988; Miehe and Miehe 1994; Tiercelin et al. 2008). The study area was described previously in detail by Lemma et al. (2020, 2019a, b). Briefly, the Bale Mountains are topographically divided into three major parts: The northern slopes (3000–3800 m. a.s.l.), the central Sanetti Plateau (3800–4377 m a.s.l), and the southern Harenna Escarpment (1400–3800 m. a.s.l.). The Sanetti Plateau is located in the center, on which the second highest peak of the country Mt. Tulu Dimtu (4377 m a.s.l.) perches (Friis 1986; Hillman 1986; Miehe and Miehe 1994). The northern slopes of the mountains are dissected by the Togona Valley, which descends towards the extensive Arsi Plateau and further down to the Great Rift Valley lowlands, which divide the country into two parts. The southern slope includes the steep Harenna Escarpment and goes down to the surrounding lowland at about 1400 m a.s.l. The vegetation shows an altitudinal zonation comprising the Afromontane forest (1450–2000 m a.s.l.), the upper montane forest dominated by *Hagenia* – *Hypericum* species (2000–3200 m a.s.l.), the Ericaceous belt (3200–3800 m a.s.l.), and the Afroalpine zone (3800–4377 m a.s.l.) being dominated by dwarf–shrubs (e.g., *Helichrysum, Alchemilla*), herbs, and grasses (mostly *Festuca*) (Hillman 1988; Woldu et al. 1989; Miehe and Miehe 1994).

The crust of the Bale Mountains is of volcanic origin, the soils which are developed from the basaltic, rhyolitic, and trachytic parent rock, can be generally characterized as silty loams of reddish–brown to black colour (Woldu et al. 1989). Nevertheless, the mountain's summit higher than 3000 m a.s.l were substantially flattened by repeated glaciations (for example between 20 and 12 cal kyr BP), the soils developed from such glacial rocks are usually shallow and gravelly (Hedberg 1964; Osmaston et al. 2005). Therefore, Andosols are the most ubiquitous soil type

but also Cambisols and Leptosols are prevalent in some parts of the Bale Mountains. In the wetland and sedimentary basin, Gleysols and Histosols, and in rock shelters, Anthrosols are also a common soil type (Yimer et al. 2006; Billi 2015).

The Bale Mountains are historically vulnerable to extreme climate changes that depict Quaternary glacier cover with a spatial extent of about 180 km^2 (Umer et al. 2004; Osmaston et al. 2005) and anthropogenic impacts (Gil-Romera et al. 2019; Ossendorf et al. 2019). The chronology of lacustrine sediment from the lake Garba Guracha (a glacial lake at 3950 m a.s.l.) dated back to the Late Glacial ($\sim$ 16.5 cal kyr BP) illustrates the presence of regional climate events, the African Humid Period (AHP), that encompasses major dry fluctuations such as Younger Dryas (YD), 6.5 cal kyr BP and 4.2 cal kyr BP (Umer et al. 2007; Bittner et al. 2020).

Currently, the climate of the Bale Mountains is characterized by 4 months (November to February) of dry season and 8 months (March to October) of wet season (Kidane et al. 2012; Lemma et al. 2020). The seasonal migration of Intertropical Convergence Zone (ITCZ) determines the present climate and rainfall patterns of the Ethiopian Highlands (Tiercelin et al. 2008). The highest annual rainfall occurs in the southwestern part (1000–1500 mm per year) and the northern part of the mountains exhibits annual rainfall ranging between 800–1000 mm per year (Miehe and Miehe 1994; Tiercelin et al. 2008). Moisture during the dry season originates primarily from the Arabian Sea, whereas during the wet season it originates primarily from the Southern Indian Ocean (Lemma et al. 2020). The Afroalpine regions of the Bale Mountains are characterized by a large diurnal temperature range of 40 °C ($-$ 15 to $+$ 26 °C) (Hedberg 1964; Hillman 1988). Even if there is a wider variability of climate in the Bale Mountains, only few records are reported. The highest mean annual temperatures in the mountains peaks range between 6 and 12 °C. At Dinsho (headquarter of the BMNP, 3170 m a.s.l.) the mean annual temperature is 11.8 °C. The lowest mean annual temperatures range from 0.6 to 10 °C with frequent frost occurring in the high peak areas during the winter season (Tiercelin et al. 2008).

Sampling

For the present study, 25 leaf samples of locally dominant plant species were collected (Fig. 1) along a southwestern and a northeastern transect (ranging from 2550 to 4377 m a.s.l. and 3870 to 4134 m a.s.l., respectively). Samples comprise *Erica trimera* (n = 5), *Erica arborea* (n = 5), *Alchemilla haumannii* (n = 5), *Festuca abyssinica* (n = 6), *Helichrysum splendidum* (n = 2), *Kniphofia foliosa* (n = 1) and *Lobelia rhynchopetalum* (n = 1). Photos illustrating the investigated plant species were previously published by Mekonnen et al. (2019). Additionally, 15 organic surface layers (= O–layers, strongly humified plant residues) and 22 mineral topsoils (= A_h–horizons, 0–10 cm soil depth) that developed under the above–listed locally dominant vegetation were collected, resulting in 62 samples in total. All samples were air–dried in the Soil Store Laboratory of the National Herbarium, Department of Plant Biology and Biodiversity Management, Addis Ababa University. In the laboratory of the Soil Biogeochemistry Group, Martin Luther University of Halle–Wittenberg, the samples were sieved using a mesh size of 2 mm, finely ground, homogenized, and subjected to further biogeochemical analysis.

Additionally, from ten newly established weather stations, we recorded hourly RH, hourly temperature, and a total of 164 precipitation samples were collected along an altitudinal transect ranging from 1304 to 4375 m a.s.l. The δ^2H_{prec} and $\delta^{18}O_{prec}$ as well as mean annual RH and temperature records above 2550 m a.s.l. were used for the present study. For more details, information regarding the spatial and temporal ^2H and ^{18}O isotope variation of the contemporary precipitation in the Bale Mountains, the readers are referred to Lemma et al. (2020).

Compound–specific $\delta^2H_{\boldsymbol{n}\text{-alkane}}$ and $\delta^{18}O_{sugar}$ analyses

Leaf wax–derived *n*-alkanes were extracted from 0.5 to 1 g of leaves, O–layers and A_h–horizons using Soxhlet extraction by adding 150 ml of dichloromethane (DCM) and methanol (MeOH) as solvents (9:1 ratio) for 24 h following a method modified after Zech and Glaser (2008). 50 µl of 5α-androstane were added to the total lipid extracts as an internal standard. Total lipid extracts were separated over aminopropyl

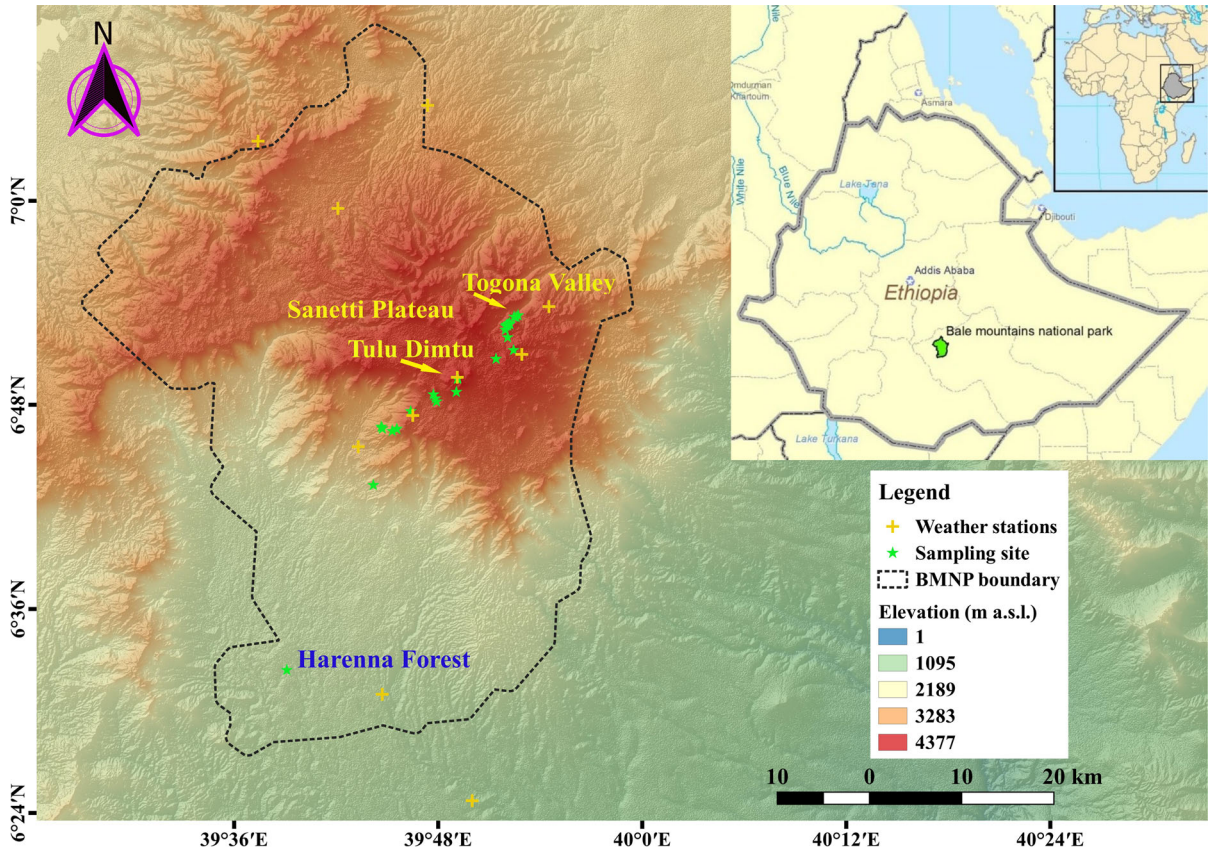

Fig. 1 Map showing the location of Ethiopia in Africa, location of the Bale Mountains National Park (BMNP) in Ethiopia, and location of sampling site (light green star) and weather stations (yellow cross) along the southwest and northeast transect in the BMNP. (Color figure online)

pipette columns (Supelco, 45 µm). Three lipid fractions containing the *n*-alkanes, alcohols, and fatty acids were eluted successively by using 3 ml of hexane, DCM/MeOH (1:1), and diethyl ether and acetic acid (95:5), respectively.

The compound–specific stable hydrogen isotope analyses of the most abundant *n*-alkanes (C_{29} and C_{31}) were determined using a Trace GC 2000 coupled to a Delta V Advantage IRMS via a thermal conversion reactor (GC IsoLink) and a ConFlo IV interface (GC–TC–IRMS, Delta V, Thermo Fisher Scientific, Bremen, Germany) operating in pyrolysis mode with reactor temperature of 1420 °C. The GC was equipped with a split/splitless injector and an Rtx–5 Sil MS column (30 m length, 0.25 mm inner dimeter, 0.5 µm film thickness). Each sample was analysed in triplicate and measurements of *n*-alkane standards (*n*-C_{27}, *n*-C_{29}, *n*-C_{33}) with known isotopic composition (Arndt Schimmelmann, Indiana) at various concentrations were embedded in–between the three sample batches. The H_3^+ factor was determined before and after each sequence and was stable at 7.57 ± 0.29 (n = 6) during the measurement campaign.

The hemicellulose–derived sugars were extracted hydrolytically (105 °C, 4 h) from aliquots of leaves, O–layers, and A_h–horizons using 10 ml of 4 M trifluoroacetic acid (TFA) following the method described by Zech and Glaser (2009). The extracted monosaccharides were purified via XAD–7 and Dowex 50WX8 resin columns as proposed by Amelung et al. (1996). For quantification, one–fifth of the freeze–dried sugar samples were derivatized using *N*-methyl-pyrrolidone (NMP) and heated for 30 min at 75 °C. After cooling, the samples were subjected for the second derivatization using 400 µl bis(trimethylsilyl) trifluoroacetamide (BSTFA) and heated again for 5 min at 75 °C. For compound–specific $\delta^{18}O_{sugar}$ analyses, the remaining four–fifth of

the samples were derivatized using the methyl–boronic acid (MBA; 4 mg in 400 µl pyridine) derivatization method and heated for 1 h at 60 °C (Zech and Glaser 2009).

The compound–specific stable oxygen isotope values were determined using a Trace GC 2000 coupled to a Delta V Advantage IRMS via an ^{18}O–pyrolysis reactor (GC IsoLink) and a ConFlo IV interface (GC–Py–IRMS, Delta V, Thermo Fisher Scientific, Bremen, Germany). The GC was equipped with a split/splitless injector and a DB– 5MS + DG column (60 m length, 0.250 mm inner dimeter, 0.25 µm film thickness). Samples were injected in splitless mode and analysed in triplicate. For calibration standard blocks of derivatised sugars (arabinose, fucose and xylose) of known isotopic composition at various concentrations were embedded in–between the six sample batches.

The measured $\delta^2H_{n\text{-alkane}}$ and $\delta^{18}O_{sugar}$ values were corrected for drift and amount–dependence, according to Zech and Glaser (2009). Out of 62 samples, five samples (four O–layers and one A_h–horizon below *Erica*) were rejected from further data evaluation and interpretation due to peak areas below detection limit. Similarly, the sugar biomarker fucose was excluded from data evaluation due to too low peak areas. Mean standard error for triplicate measurements of the remaining 57 samples are 0.8‰, 0.9‰, 3.1‰, 2.3‰ for arabinose, xylose, *n*-C_{29}, and *n*-C_{31} alkanes, respectively. The standard errors for the sugar and *n*-alkane standards were 2‰ (n = 22) and 5‰ (n = 28), respectively. In the following, $\delta^2H_{n\text{-alkane}}$ values refer to weighted mean values of *n*-C_{29} and *n*-C_{31}, and $\delta^{18}O_{sugar}$ values refer to weighted mean values of arabinose and xylose. The weighted mean for $\delta^2H_{n\text{-alkane}}$ and $\delta^{18}O_{sugar}$ values were calculated using the relative amounts of *n*-C_{29} and *n*-C_{31} as well as arabinose and xylose, respectively. The $\delta^2H_{n\text{-alkane}}$ and $\delta^{18}O_{sugar}$ values are reported in per mil (‰) according to the usual δ–notation relative to Vienna Standard Mean Ocean Water (V–SMOW) given in Eq. 1.

$$\delta = \left(R_{sample}/R_{standard} - 1\right) \times 10^3 \quad (1)$$

where R refers to the ratio of $^{18}O/^{16}O$ and $^2H/^1H$ for the sample or standard (V–SMOW) materials.

Conceptual framework for interpreting the coupled $\delta^2H_{n\text{-alkane}}$–$\delta^{18}O_{sugar}$ approach: reconstruction of leaf water, source water, *d*-excess, and relative humidity

The isotopic composition of leaf water ($\delta^2H_{leaf\ water}$ and $\delta^{18}O_{leaf\ water}$) can be reconstructed from the isotopic composition of biomarkers ($\delta^2H_{n\text{-alkane}}$ and $\delta^{18}O_{sugar}$) by subtracting biosynthetic fractionation factors (Zech et al. 2013b; Tuthorn et al. 2015; Hepp et al. 2017, 2019). Apart from assuming that the biosynthetic fractionation factors (ε_{bio}) are constant and not significantly variable amongst plants, we assume moreover that both biomarkers (sugars and *n*-alkanes) are primarily leaf–derived. We acknowledge that both assumptions are valid only in approximation. We apply ε_{bio} of − 160‰ (Sessions et al. 1999) to reconstruct $\delta^2H_{leaf\ water}$ (Eq. 2) and + 27‰ (Sternberg 1989; Schmidt et al. 2001; Cernusak et al. 2003; Gessler et al. 2009) to reconstruct $\delta^{18}O_{leaf\ water}$ (Eq. 3). These values were recently validated by Hepp et al. (2020b) using a dataset obtained from a well–controlled climate chamber experiment.

$$\delta^{18}O_{leafwater} = \left(\delta^{18}O_{sugar} - \varepsilon^{18}_{bio}\right)/\left(1 + \varepsilon^{18}_{bio}/1000\right) \quad (2)$$

$$\delta^2H_{leaf\ water} = \left(\delta^2H_{n-alkane} - \varepsilon^{2}_{bio}\right)/\left(1 + \varepsilon^{2}_{bio}/1000\right) \quad (3)$$

Once the isotopic composition of leaf water is calculated according to Eqs. 2 and 3, it is possible to reconstruct the isotopic composition of source water, *d*-excess and RH according to Eqs. (4), (5), and (6), respectively.

Leaf water becomes ^2H– and ^{18}O–enriched due to evapotranspiration via stomata and will reach isotope steady–state under constant environmental conditions. This process is accompanied by equilibrium and kinetic isotope effects. The isotopic composition of $\delta^2H_{leaf\ water}$ and $\delta^{18}O_{leaf\ water}$ then depends primarily on RH, the isotopic composition of source water and the isotopic composition of atmospheric water vapor (Dongmann et al. 1974; Flanagan et al. 1991; Roden and Ehleringer 1999). Once isotope steady–state is achieved, the isotope ^2H– and ^{18}O–enrichment of leaf water can be described using a Craig–Gordon model (Craig and Gordon 1965) adapted by Gat and Bowser (1991) and later by Zech et al. (2013b). The isotopic

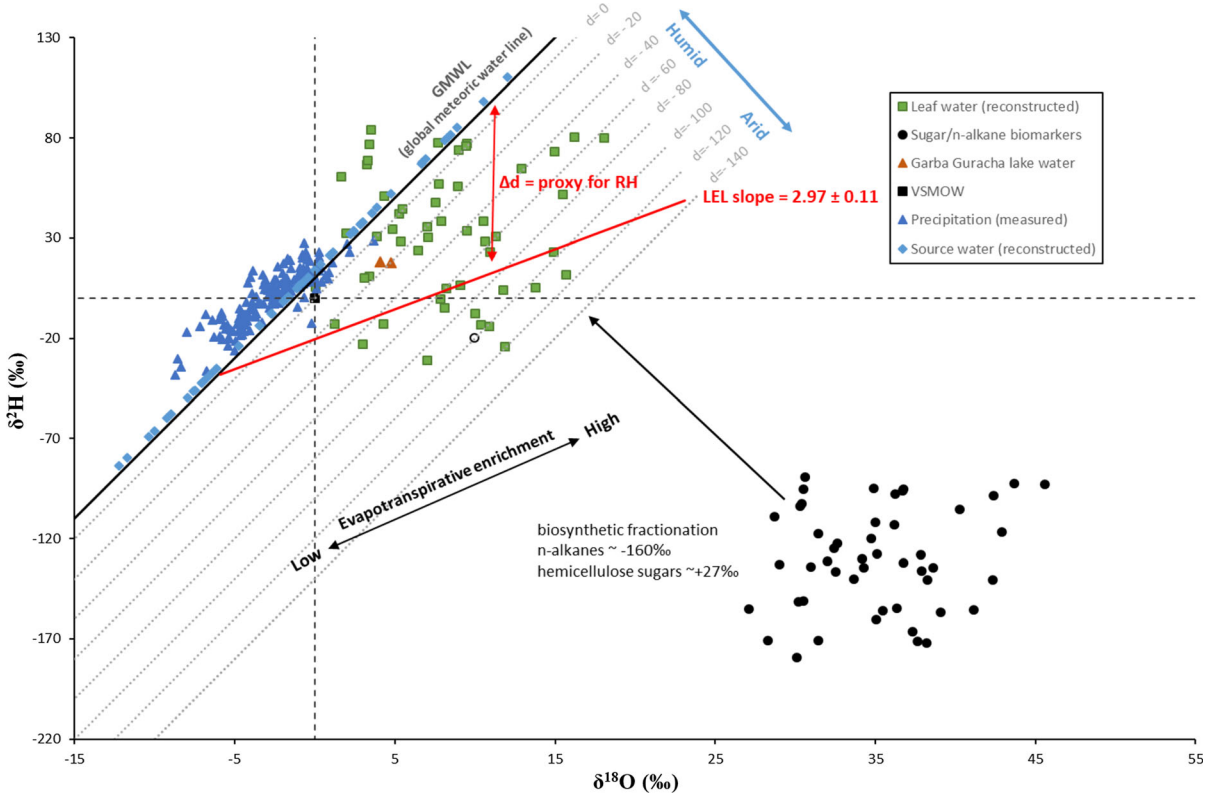

Fig. 2 $\delta^{18}O$ versus $\delta^{2}H$ diagram illustrating the conceptual framework of the coupled (paleo–) hygrometer approach after Zech et al. (2013b). Data are plotted for measured precipitation (blue solid triangle), measured $\delta^{2}H_{n\text{-alkane}}$, and $\delta^{18}O_{sugar}$ biomarkers (black solid circle), reconstructed leaf water (green solid rectangle), reconstructed source water (light blue solid rectangle), measured Garba Guracha lake water (brown solid triangle), global meteoric water line, GMWL (black solid line) and local evaporation line, LEL (red solid line). (Color figure online)

composition of leaf water at the evaporative site can be calculated using Eq. 4.

$$\delta_{leafwater} = \delta_{sourcewater} + (1 - RH)\varepsilon^{*} + \Delta\varepsilon \quad (4)$$

where $\delta_{leaf\ water}$ and $\delta_{source\ water}$ are the isotopic composition of leaf water and source water, respectively, RH is relative humidity, ε^{*} is equilibrium isotope enrichment ($(1 - 1/\alpha_{L/V}) * 10^{3}$), and $\Delta\varepsilon$ is kinetic isotope enrichment [$\Delta^{18}\varepsilon = C_k^{18}(1 - RH)$; $\Delta^{2}\varepsilon = C_k^{2}(1 - RH)$]. C_k^{18} and C_k^{2} are kinetic isotope enrichment constants for ^{18}O and ^{2}H, respectively.

In a two–dimensional $\delta^{2}H$–$\delta^{18}O$ diagram, the isotope values of precipitation plot along the GMWL (Craig 1961; Dansgaard 1964), whereas due to transpiration leaf water becomes ^{2}H– and ^{18}O–enriched compared to source water (precipitation) (Farquhar et al. 2007; Feakins and Sessions 2010) and the isotope values of leaf water plot along the evaporation line (Zech et al. 2013b; Tuthorn et al. 2015). The distance of the reconstructed leaf water to the GMWL can be described as *d*-excess and serves as a proxy for relative humidity (Fig. 2). *d*-excess is a second– order stable isotope parameter measured in meteoric water defined as $d\text{-excess} = \delta^{2}H - 8*\delta^{18}O$. Therefore, *d*-excess of leaf water can be derived using Eq. 5.

$$d_{leaf\ water} = d_{source\ water} + (1 - RH)\left(\varepsilon_2^{*} - 8 * \varepsilon_{18}^{*} + C_k^{2} - 8 * C_k^{18}\right) \quad (5)$$

where $d_{leaf\ water}$ and $d_{source\ water}$ are *d*-excess of leaf water and source water, respectively and the equilibrium (ε_2^{*} and ε_{18}^{*}) and kinetic (C_k^{2} and C_k^{18}) isotope fractionation of the two isotopes. Equation 5 illustrates that *d*-excess depends primarily on RH. Therefore, RH normalized to the temperature of leaf water can be estimated using Eq. 6.

$$RH \approx 1 - \frac{\Delta d}{\left(\varepsilon_2^* - 8 * \varepsilon_{18}^* + C_k^2 - 8 * C_k^{18}\right)} \quad (6)$$

where Δd is the difference between d-excess of leaf water and d-excess of source water. Equilibrium isotope fractionation factors (ε_2^* and ε_{18}^*) as a function of temperature are calculated according to empirical equations of Horita and Wesolowski (1994). According to Merlivat (1978), the maximum values of kinetic isotope fractionation factors (C_k^2 and C_k^{18}) during molecular diffusion of water via a stagnant air for ^2H and ^{18}O are 25.1‰ and 28.5‰, respectively. However, we are aware that the kinetic isotope fractionation factors are dependent on aerodynamic conditions (liquid–vapor interface, diffusive, and turbulent layer) characterising a given evaporation process.

The values of $\delta^2H_{source\ water}$ and $\delta^{18}O_{source\ water}$ can be estimated when the slope of the evaporation line for leaf water is known. The slope of the evaporation line can be derived from Eq. 7.

$$S_{LEL} = \frac{\delta_e^2 - \delta_s^2}{\delta_e^{18} - \delta_s^{18}} \approx \frac{\varepsilon_2^* + C_k^2}{\varepsilon_{18}^* + C_k^{18}} \quad (7)$$

In this equation, we assumed that the isotopic composition of source water and atmospheric water vapor reached equilibrium. Thus, the slope of the evaporation line depends on equilibrium (ε_2^* and ε_{18}^*) and kinetic (C_k^{18} and C_k^2) isotope fractionation factors of the two isotopes (Gat and Bowser 1991). In the present study, the slope of the local evaporation line (LEL) ranges between 2.86 and 3.07 ($\bar{x}$ = 2.97 ± 0.11) for the temperature ranging between 3.2 and 12.7 °C. Here in this manuscript, ± sign refer to standard error values. Such low slope for evaporating leaf water is in agreement with both field observations and laboratory experiments (Allison et al. 1985; Walker and Brunel 1990; Gat et al. 2007).

The net isotope difference (also called apparent fractionation, ε_{app}) between $\delta^2H_{n\text{-alkane}}$ and δ^2H_{prec} as well as $\delta^{18}O_{sugar}$ and $\delta^{18}O_{prec}$ is calculated using Eq. 8.

$$\varepsilon_{app} = 1000 \times \left(\frac{\delta_a + 1000}{\delta_b + 1000} - 1\right) \quad (8)$$

where a is the isotopic composition of a biomarker ($\delta^2H_{n\text{-alkane}}$ or $\delta^{18}O_{sugar}$) and b is the weighted mean annual isotopic composition of precipitation (δ^2H_{prec} or $\delta^{18}O_{prec}$).

Results and discussion

Comparison of $\delta^2H_{n\text{-alkane}}$ and $\delta^{18}O_{sugar}$ results from leaves, O–layers, and A_h–horizons

The δ^2H values of n-C_{29} and n-C_{31} alkanes as well as the $\delta^{18}O$ values of arabinose and xylose correlate highly significant with each other ($r = 0.9$, $p < 0.0001$ and $r = 0.8$, $p < 0.0001$, respectively, ESM_1 and 2 of the supplementary files). In the following, we therefore use and refer to $\delta^2H_{n\text{-alkane}}$ values for weighted mean values of n-C_{29} and n-C_{31} as well as to $\delta^{18}O_{sugar}$ values for weighted mean values of arabinose and xylose. Weighted mean $\delta^2H_{n\text{-alkane}}$ and $\delta^{18}O_{sugar}$ values range from − 186 to − 89‰ and from + 27 to + 46‰, respectively (Fig. 3). Particularly, the topsoil (O–layer as well as A_h–horizon) samples in the Bale Mountains yielded a $\delta^2H_{n\text{-alkane}}$ values range between − 157 and − 113‰ ($\bar{x}$ = − 136‰), which is in good agreement with findings from the highest Eastern African Mt. Kilimanjaro (Peterse et al. 2009; Zech et al. 2015; Hepp et al. 2017), Mt. Rungwe and Mt. Kenya (Coffinet et al. 2017).

The $\delta^2H_{n\text{-alkane}}$ and $\delta^{18}O_{sugar}$ values of leaves, O–layers, and A_h–horizons do not depict statistically significant differences ($p = 0.7$ and $p = 0.4$, respectively) among each other (Fig. 4a and b). Hence, our data provide no evidence for degradation effects affecting the isotopic composition of the biomarkers. Similarly, there is no evidence for root and soil microbial–derived n-alkanes and sugars affecting the compound–specific hydrogen and oxygen isotope signals. This is remarkable because our previous chemotaxonomy studies reveal that the characteristic plant biomarker patterns of long-chain n-alkanes and sugars are strongly altered in the respective O–layers and A_h–horizons due to degradation and/or underground input by roots (Lemma et al. 2019b; Mekonnen et al. 2019).

Concerning $\delta^{18}O_{sugar}$, Zech et al. (2012b) reported the absence of isotope fractionation during decomposition based on a litter decay study. By contrast, based on the same litter decay sample set, Zech et al. (2011) concluded that the built-up of a microbial n-alkane pool can change the $\delta^2H_{n\text{-alkane}}$ values of soils compared to litter. The same conclusion was drawn by Tu et al. (2011) based on a $\delta^{13}C$ n-alkane litter decay study. A possible explanation for this

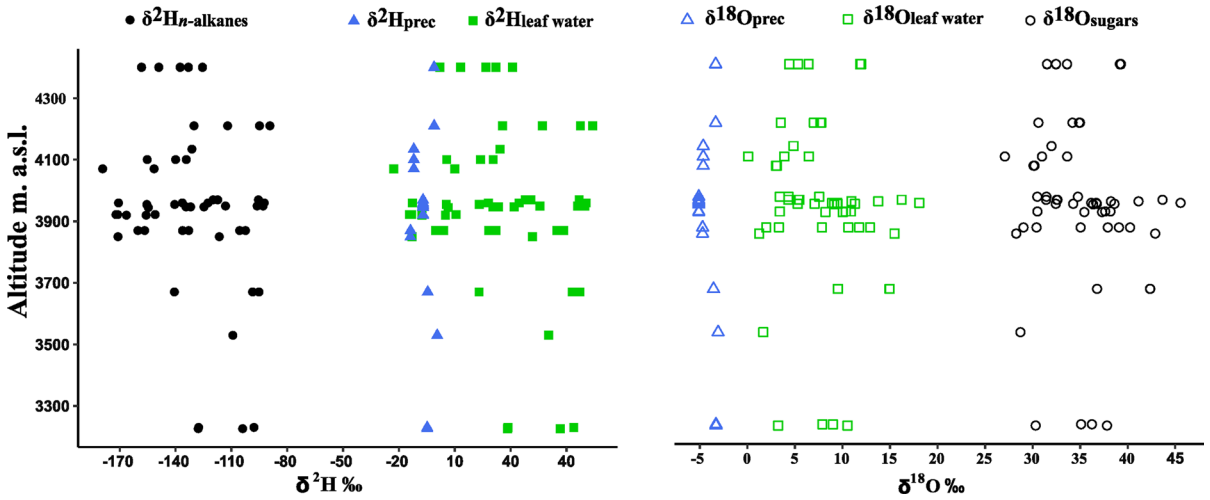

Fig. 3 Altitudinal δ^2H (left) and $\delta^{18}O$ (right) gradients of *n*-alkanes (weighted mean of *n*-C_{29} and *n*-C_{31}, solid circles) and sugars (weighted mean of arabinose and xylose, empty circles), respectively, reconstructed leaf water (squares) of all the investigated samples as well as measured weighted mean annual precipitation (triangles)

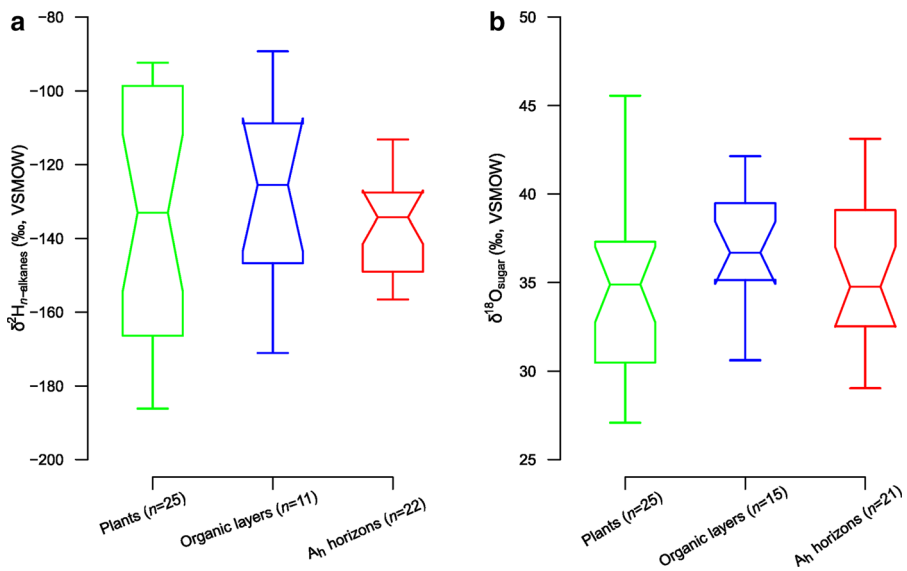

Fig. 4 Comparison of $\delta^2H_{n\text{-alkane}}$ (**a**) and $\delta^{18}O_{sugar}$ (**b**) among leaves, O–layers and A_h–horizons. The notched box plots indicate the median (solid lines between the boxes), interquartile range (IQR) with upper (75%) and lower (25%) quartiles. The notches display the confidence interval around the median within $\pm$ 1.57*IQR/$\sqrt{n}$

discrepancy could be that $\delta^2H_{n\text{-alkane}}$ and $\delta^{18}O_{sugar}$ variability in our dataset are very large within the leaf, O– layer, and A_h–horizon sub-dataset (Fig. 4a and b). Indeed, albeit not significant, the median values of O–layers reveal both the least negative $\delta^2H_{n\text{-alkane}}$ and the most positive $\delta^{18}O_{sugar}$. It is noteworthy that the concentration of *n*-alkanes in roots is much lower than in leaves and the contamination of leaf wax–derived *n*-alkanes in sediment by the roots is negligible (Zech et al. 2012a, 2013a), whereas a partial contribution of especially root–derived sugars to O–layers and A_h–horizons is very likely. Still, the mean $\delta^2H_{n\text{-alkane}}$ and $\delta^{18}O_{sugar}$ values of leaves and A_h–horizons are almost identical (− 134 versus − 135‰ and 35 versus 36‰, respectively). Hence, our dataset does not provide

evidence for degradation effects and root input affecting $\delta^2H_{n\text{-alkane}}$ and $\delta^{18}O_{sugar}$ values of topsoils.

Comparison of $\delta^2H_{n\text{-alkane}}$ and $\delta^{18}O_{sugar}$ results with δ^2H_{prec} or $\delta^{18}O_{prec}$ results

The $\delta^2H_{n\text{-alkane}}$ values correlate significantly with the weighted mean annual isotopic composition of local meteoric water, δ^2H_{prec} ($r = 0.3$, $p = 0.04$, n = 53, ESM_3 of the supplementary files). However, it does not correlate in a 1:1 relationship ($\delta^2H_{prec} = 0.05*\delta^{2}H_{n\text{-alkane}} - 1.03$) and this is the first important indication that *n*-alkanes do not directly reflect δ^2H_{prec}. Instead, $\delta^2H_{n\text{-alkane}}$ reflects the isotope signal of local precipitation modified by leaf water enrichment as emphasized by Zech et al. (2015). The isotopic composition of precipitation in the Bale Mountains is subjected to altitude, amount, and seasonal effects. The most positive δ^2H_{prec} and $\delta^{18}O_{prec}$, as well as the more negative δ^2H_{prec} and $\delta^{18}O_{prec}$ values, were recorded in the lowermost and highest weather stations of the Bale Mountains, respectively (Lemma et al. 2020). However, the overall significant trend of the altitudinal effect observed in modern precipitation is not well reflected in the $\delta^2H_{n\text{-alkane}}$ and $\delta^{18}O_{sugar}$ (Fig. 3). Our findings are hence in agreement with $\delta^2H_{n\text{-alkane}}$ results from Mt. Kilimanjaro (Peterse et al. 2009; Zech et al. 2015), Mt. Rungwe (Coffinet et al. 2017) and the southwest Ethiopian highlands (Jaeschke et al. 2018). There is also no significant correlation between $\delta^{18}O_{sugar}$ and $\delta^{18}O_{prec}$ in our dataset. This might indicate that the isotope signal of $\delta^{18}O_{prec}$ is strongly altered prior to the biosynthesis of the sugar biomarkers. Thus, soil water evaporation, leaf water evapotranspiration and seasonality effects are the most likely responsible factors. A recent publication by Strobel et al. (2020) argued that plant–related and/or environmental factors strongly bias the $\delta^{18}O_{sugar}$ signal compared to $\delta^{18}O_{prec}$ and points especially to the significant impact of evapotranspirative soil and leaf water enrichment. Similarly, a climate transect study revealed that $\delta^{18}O_{hemicellulose}$ does not reflect $\delta^{18}O_{prec}$ along an Argentinian transect, either (Tuthorn et al. 2014). Overall it can be summarized that our $\delta^2H_{n\text{-alkane}}$ and $\delta^{18}O_{sugar}$ values do not directly reflect the isotopic composition of precipitation in the Bale Mountains.

The apparent isotope fractionation (ε_{app}) for each investigated plant species (only leaf samples) ranges for hydrogen ($\varepsilon_{app\ 2H}$) between − 180 to − 86‰ and for oxygen ($\varepsilon_{app\ 18O}$) between + 25 to + 56‰. The ε_{app} factors fundamentally depend on three processes (Fig. 5, after Strobel et al. 2020). Accordingly, the main processes influencing the imprint of precipitation isotope on biomarkers are soil–water evaporation, leaf–water transpiration, and biosynthetic fractionation. The mean $\varepsilon_{app\ 2H}$ and $\varepsilon_{app\ 18O}$ values of the investigated plant species in the Bale Mountains are − 128 ± 6‰ and + 40 ± 2‰, respectively. This is in a good agreement and within the range of results reported from a winter rainfall zone transect study in South Africa (Strobel et al. 2020).

In the present study, there is no significant correlation between apparent isotope fractionation and mean day time temperature ($\varepsilon_{app\ 18O}$, $r = 0.1$, $p = 0.5$ and $\varepsilon_{app\ 2H}$, $r = 0.3$, $p = 0.1$). Thus, the apparent isotope fractionation is not influenced by temperature–related evapotranspirative enrichment. This is in agreement with the results of Strobel et al. (2020) who found that neither $\varepsilon_{app\ 2H}$ nor $\varepsilon_{app\ 18O}$ is significantly dependent on mean annual temperature (MAT).

Interspecies comparison of $\delta^2H_{n\text{-alkane}}$ and $\delta^{18}O_{sugar}$ results from dominant plant species in the Bale Mountains

Combining all leaf, O–layer and A_h–horizon data, the comparison of the $\delta^2H_{n\text{-alkane}}$ values between the plant species under study depicts significant differences (Fig. 6a). More specifically, *Erica arborea* and *Erica trimera* yielded the least negative median $\delta^2H_{n\text{-alkane}}$ values, whereas *Festuca abyssinica* yielded the most negative median $\delta^2H_{n\text{- alkane}}$ value (Fig. 6a). Albeit the $\delta^{18}O_{sugar}$ values show no significant difference amongst the dominant plant species (Fig. 6b), they reveal the same trends as the $\delta^2H_{n\text{-alkane}}$ results. Particularly, *E. arborea* and *E. trimera* depicted the most positive median $\delta^{18}O_{sugar}$ values, whereas *F. abyssinica* depicted the least positive median $\delta^{18}O_{sugar}$ value (Fig. 6b). The mean $\delta^2H_{n\text{-alkane}}$ and $\delta^{18}O_{sugar}$ values of *E. arborea* and *E. trimera* are − 114 and − 109‰, and + 37 and + 36‰, respectively. These very close mean $\delta^2H_{n\text{-alkane}}$ and $\delta^{18}O_{sugar}$ values of the two *Erica* species likely reflect the monophyletic nature (Guo et al. 2014).

One might expect that the above described plant–specific differences can be explained with the altitude–

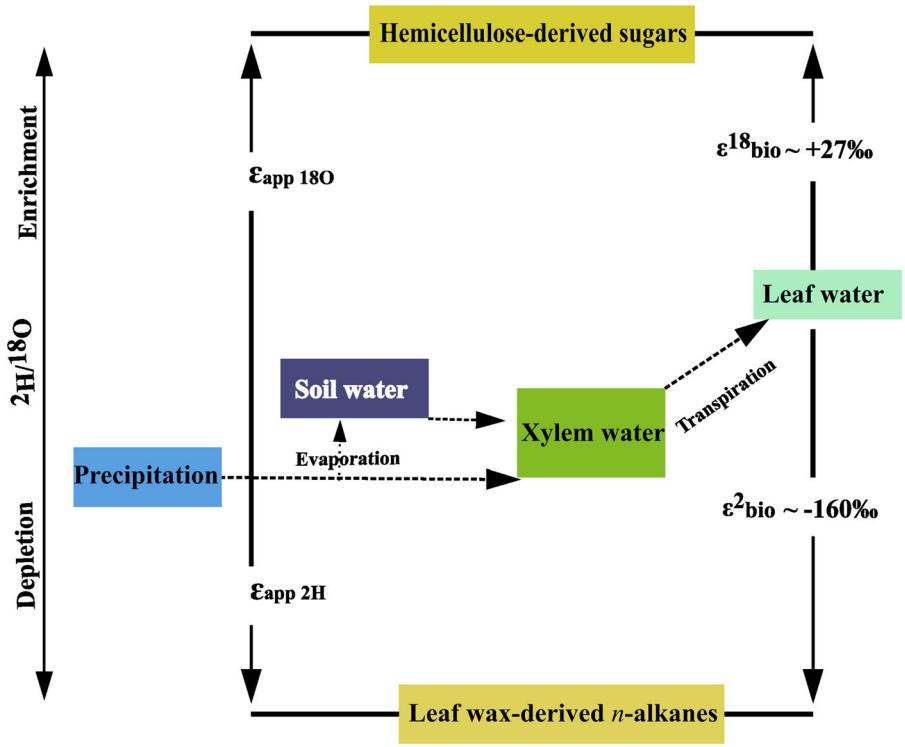

Fig. 5 Conceptual model demonstrating the hydrogen–isotope and oxygen–isotope relationships, between precipitation, leaf water, and leaf wax–derived *n*-alkanes as well as hemicellulose–derived sugars (after Strobel et al. 2020). $\varepsilon_{app\ 2H}$: apparent hydrogen-isotope fractionation, $\varepsilon_{app\ 18O}$: apparent oxygen-isotope fractionation, ε^{18}_{bio}: biosynthetic oxygen–isotope fractionation, ε^{2}_{bio}: biosynthetic hydrogen-isotope fractionation

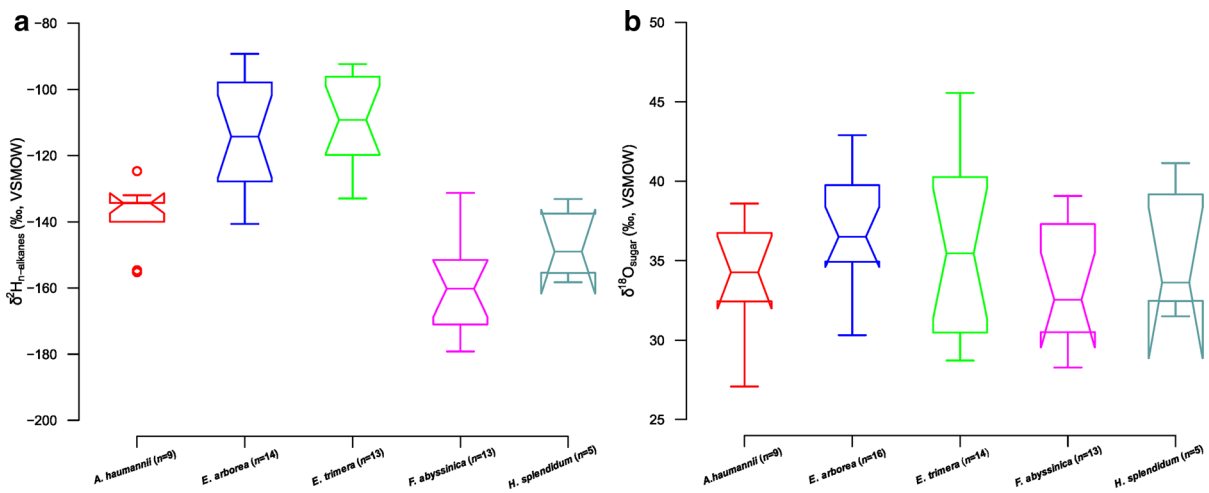

Fig. 6 Variations of $\delta^2H_{n\text{-alkane}}$ (**a**) and $\delta^{18}O_{sugar}$ (**b**) between samples (leaf, O–layer and A_h–horizon) of the dominant plant species. The notched box plots indicate the median (solid lines between the boxes), interquartile range (IQR) with upper (75%), and lower (25%) quartiles and outliers (empty circle). The notches display the confidence interval around the median within $\pm$ 1.57*IQR/$\sqrt{n}$

dependent different occurrence of the investigated plant species and altitude–dependent δ^2H_{prec} and $\delta^{18}O_{prec}$ variability. Indeed, the δ^2H_{prec} and $\delta^{18}O_{prec}$ values in the Bale Mountains exhibit spatial variance along the altitudinal gradient with isotope lapse rates of − 0.52‰*100 m^{-1} and − 0.11‰*100 m^{-1}, respectively (Lemma et al. 2020). This corresponds roughly to a range of 5 and 1‰ for δ^2H_{prec} and $\delta^{18}O_{prec}$, respectively, along the investigated altitudinal transect (3226 and 4375 m a.s.l.). These ranges are, however, too small to explain the observed large $\delta^2H_{n\text{-alkane}}$ and $\delta^{18}O_{sugar}$ variability along the transect (Fig. 3). Strikingly, the median $\delta^2H_{n\text{-alkane}}$ and $\delta^{18}O_{sugar}$ values of *F. abyssinica* are the lowest compared to the other investigated plant species. This can be attributed to physiological and biochemical differences and the fact that *F. abyssinica* (grass) is a monocot, whereas the other plant species are dicots. The leaves of monocots and dicots differ in structure, location and timing of lipid synthesis (Sachse et al. 2012). The growth of grasses is associated with intercalary meristems. They occur at the base of the grass leaf blade, where leaf water is not fully ^2H– and ^{18}O–enriched. Thus, newly synthesized lipids and sugars at the base of grass leaves do not incorporate the full leaf water enrichment signal, which is called $^2H_{n\text{-alkane}}$ and $^{18}O_{sugar}$ "signal–damping or dampening effect" (Hepp et al. 2019, 2020a). On the other hand, the median $\delta^2H_{n\text{-alkane}}$ and $\delta^{18}O_{sugar}$ values of *E. arborea* and *E. trimera* are the highest in comparison with other species and show strong leaf water enrichment. The intermediate $\delta^2H_{n\text{-alkane}}$ and $\delta^{18}O_{sugar}$ values for *A. haumannii* and *H. splendidum* might be attributed to plant physiological and biochemical differences or microclimatic conditions affecting RH values and thus leaf water enrichment as compared to *Erica* and *F. abyssinica*.

Furthermore, there is a significant difference in $\varepsilon_{app\ 2H}$ between the dominant plant species in the Bale Mountains. Unlike other species, *E. arborea* (− 94‰) and *E. trimera* (− 92‰) have the least negative and *F. abyssinica* (− 161‰) has the most negative $\varepsilon_{app\ 2H}$. It is known that C3 graminoid (Sachse et al. 2012) and C3 grasses (Gamarra et al. 2016) exhibited the most negative $\varepsilon_{app\ 2H}$ compared to shrubs and trees. Such species–dependent variation of $\varepsilon_{app\ 2H}$ can be attributed to intrinsic factors (e.g., plant physiological, phenological, photosynthesis pathway and biosynthesis–related), plant growth form, place and timing of leaf–wax synthesis, and stomatal nature (Liu and Yang 2008; Sachse et al. 2012; Gao et al. 2015; Griepentrog et al. 2019; Strobel et al. 2020). Therefore, caution must be given in terms of vegetation change when interpreting $\delta^2H_{n\text{-alkane}}$ for paleoclimate reconstruction. There is no significant difference in $\varepsilon_{app\ 18O}$ among dominant plant species in the Bale Mountains and *H. splendidum* shows the least positive $\varepsilon_{app\ 18O}$ value (26‰). This finding might demonstrate that $\varepsilon_{app\ 18O}$ is not strongly sensitive to vegetation type rather climate–related evapotranspirative enrichment. Previous studies of Tuthorn et al. (2014) and Strobel et al. (2020) described $\delta^{18}O_{sugar}$ and $\varepsilon_{app\ 18O}$ are significantly influenced by evapotranspiration and aridity index.

Coupled $\delta^2H_{n\text{-alkane}}$ and $\delta^{18}O_{sugar}$ biomarker results

Reconstructed $\delta^2H_{leaf\ water}$ and $\delta^{18}O_{leaf\ water}$ as well as $\delta^2H_{source\ water}$ and $\delta^{18}O_{source\ water}$

The basic principle of the coupled $\delta^2H_{n\text{-alkane}}$ – $\delta^{18}O_{sugar}$ approach is based on the assumption that long–chain *n*-alkanes and pentose sugars are leaf–derived and reflect the isotopic composition of leaf water (Zech et al. 2013b, 2015; Tuthorn et al. 2015; Hepp et al. 2017, 2019). The isotopic composition of reconstructed leaf water is determined by the isotopic composition of local precipitation and evaporative leaf water enrichment. However, soil–water enrichment cannot be excluded but is considered to be negligible. Therefore, the reconstructed $\delta^2H_{leaf\ water}$ and $\delta^{18}O_{leaf\ water}$ allow us to reconstruct $\delta^2H_{source\ water}$ and $\delta^{18}O_{source\ water}$ as well as *d*-excess and RH. These valuable proxies and additional information can support a better understanding of the paleoclimate history, which cannot be addressed by a single isotope study. The reconstructed $\delta^2H_{leaf\ water}$ and $\delta^{18}O_{leaf\ water}$ values range between − 31 to 84‰ ($\bar{x}$ = 31 ± 4‰) and 0.1 to 18‰ ($\bar{x}$ = 8 ± 0.6‰), respectively (Fig. 3). Most of the reconstructed leaf water data plot below the GMWL (Fig. 2). The reconstructed leaf water data plotting below the GMWL is a typical feature of evaporation loss.

By applying a biosynthetic fractionation factor of − 160‰, the reconstructed $\delta^2H_{leaf\ water}$ values highlight that the *n*-alkanes of *F. abyssinica* (Fig. 6a) reflect quite accurately and precisely the weighted

mean annual δ^2H_{prec} (− 2.7 ± 2‰) of the Bale Mountains (Lemma et al. 2020). However, it is known that the effect of evaporative leaf water isotope enrichment of grasses is negligible (Helliker and Ehleringer 2002; McInerney et al. 2011). By contrast, the reconstructed $\delta^2H_{leaf\ water}$ values of *E. arborea* and *E. trimera* (Fig. 6a) do not reflect accurately and precisely the weighted mean annual δ^2H_{prec} and the reconstructed $\delta^2H_{leaf\ water}$ is higher compared to δ^2H_{prec} by up to + 55 ± 5‰ (Fig. 6a). One well known and widely accepted factor responsible for this finding is leaf water enrichment. For instance, Zech et al. (2015) emphasized that $\delta^2H_{n\text{-alkane}}$ data from a climate transect along the southern slopes of Mt. Kilimanjaro do not reflect δ^2H_{prec} either and explained this with a strongly variable degree of leaf water enrichment along the altitudinal transect. Hence, our datasets clearly indicate that unlike *Erica* (dicots), the reconstructed $\delta^2H_{leaf\ water}$ of *F. abyssinica* (monocot) does not fully expose to evaporative leaf water enrichment due to signal–dampening.

Similarly, considering a biosynthetic fractionation factor of + 27‰ (Cernusak et al. 2003), the reconstructed $\delta^{18}O_{leaf\ water}$ values of all investigated plant species (Fig. 6b) do not reflect the isotopic composition of precipitation, $\delta^{18}O_{prec}$ (− 3.3 ± 0.4‰) in the Bale Mountains (Lemma et al. 2020). More specifically, the reconstructed $\delta^{18}O_{leaf\ water}$ values of *E. arborea* and *E. trimera* are higher compared to $\delta^{18}O_{prec}$ by up to + 9 ± 1‰ (Fig. 6b). Indeed, yet it is not significant, the reconstructed $\delta^{18}O_{leaf\ water}$ is also species–dependent. Tree ring research has shown that cellulose does not reflect the full leaf water $\delta^{18}O$ enrichment signal (Gessler et al. 2013). Additionally, results from climate chamber experiments indicate that $\delta^{18}O_{leaf\ water}$ values, reconstructed from sugar biomarker, are more positive compared to plant source water by up to + 25‰ (Zech et al. 2014a).

Moreover, the coupled $\delta^2H_{n\text{-alkane}}$ –$\delta^{18}O_{sugar}$ approach allows us to reconstruct the isotopic composition of source water as intersect of the local evaporation line (LEL) with the GMWL (Fig. 2). The reconstructed $\delta^2H_{source\ water}$ and $\delta^{18}O_{source\ water}$ values range from − 84 to 110‰ ($\bar{x}$ = 8.6 ± 7‰) and − 12 to 12‰ ($\bar{x}$ = − 0.7 ± 0.8‰) (Figs. 2 and 7), respectively. Unlike δ^2H_{prec} and $\delta^{18}O_{prec}$, the reconstructed $\delta^2H_{source\ water}$ and $\delta^{18}O_{source\ water}$ shows a large scattering (Fig. 7). The mean reconstructed $\delta^2H_{source\ water}$ and $\delta^{18}O_{source\ water}$ values reveal slight isotope enrichment as compared with the modern–day isotopic composition of δ^2H_{prec} (− 2.7 ± 2‰) and $\delta^{18}O_{prec}$ (− 3.3 ± 0.4‰) in the Bale Mountains, respectively (Lemma et al. 2020). Despite the large scattering of the reconstructed source water values this finding demonstrates that the coupled $\delta^2H_{n\text{-alkane}}$ –$\delta^{18}O_{sugar}$ approach allows to reconstruct the isotopic composition of source water quite accurately.

The correlation and offsets between the reconstructed source water and respective $\delta^{18}O_{prec}$ as well as δ^2H_{prec} are shown in Fig. 7. The offsets between the reconstructed source water and respective $\delta^{18}O_{prec}$ and δ^2H_{prec} show a highly significant difference (p = 0.001, n = 53) among the investigated plant species (box plots of Fig. 7). The median offset of *F. abyssinica* ($\delta^{18}O$ = − 3‰; δ^2H = − 33‰) and *H. splendidum* ($\delta^{18}O$ = − 3‰; δ^2H = − 36‰) are very close to each other and *E. trimera* ($\delta^{18}O$ = 8‰; δ^2H = 48‰) exhibits a markedly larger median offset than the other species (Fig. 7).

Deuterium excess, reconstructed relative humidity and its paleoclimate implication

The distance between the reconstructed leaf water and GMWL can be described as *d*-excess, which is the intercept of the meteoric water line (Dansgaard 1964), and serves as a proxy for RH (Hepp et al. 2017, 2019). The reconstructed *d*-excess values calculated using Eq. (5) range between − 105 and + 56‰. The most positive reconstructed *d*-excess values are likely caused by an overestimation of the δ^2H and/or an underestimation of the $\delta^{18}O$ values. Similarly, the most negative reconstructed *d*-excess values are likely caused by an underestimation of the δ^2H and/or an overestimation of the $\delta^{18}O$ values. The actual RH ranges between 69 and 82% ($\bar{x}$ = 80 ± 3.4%) (Fig. 8). The reconstructed RH calculated using Eq. (6) reveals a much wider range of 40 to 121% ($\bar{x}$ = 78 ± 21%), with eight anomalous values above 100% (Fig. 8). These anomalies can be explained by several uncertainties related to Δd, ε^*, and C_k values used in Eq. (6). The uncertainties of Δd mainly arise from analytical errors associated with the individual $\delta^2H_{n\text{-alkane}}$ and $\delta^{18}O_{sugar}$ measurement as well as uncertainties of the ε_{bio}. In approximation, the coupled approach of Zech et al. (2013b) suggests temperature–independent constant ε_{bio} values. However, concerning e.g. $\delta^{18}O$, this value is very likely an underestimation. Slightly higher

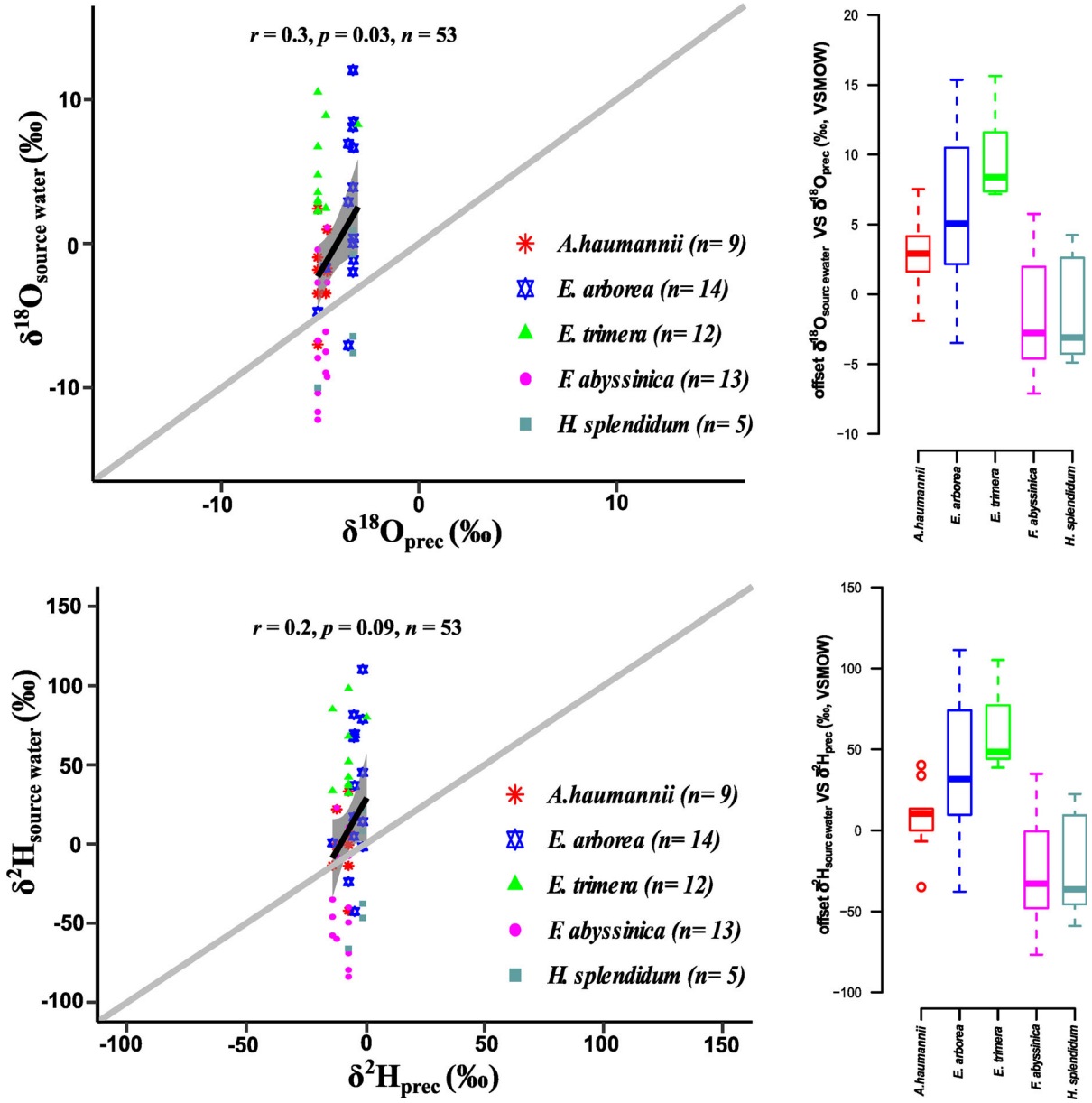

Fig. 7 The scatter plots to the left show the correlations between $\delta^{18}O_{source\ water}$ (reconstructed) and $\delta^{18}O_{prec}$ (measured) as well as $\delta^{2}H_{source\ water}$ (reconstructed) and $\delta^{2}H_{prec}$ (measured), respectively. The linear regression lines (black line), correlation coefficients (*r*), 95% confidence intervals (grey area) and significance values (*p*) as well as the 1:1 regression lines (grey lines) are provided for each diagram. The box plots to the right illustrate the offset of $\delta^{18}O_{source\ water}$ (reconstructed) to $\delta^{18}O_{prec}$ (measured) and $\delta^{2}H_{source\ water}$ (reconstructed) to $\delta^{2}H_{prec}$ (measured), respectively for the dominant plant species. The plots indicate the median (solid line between the boxes), interquartile range (IQR) with upper (75%) and lower (25%) quartiles and outliers (circles)

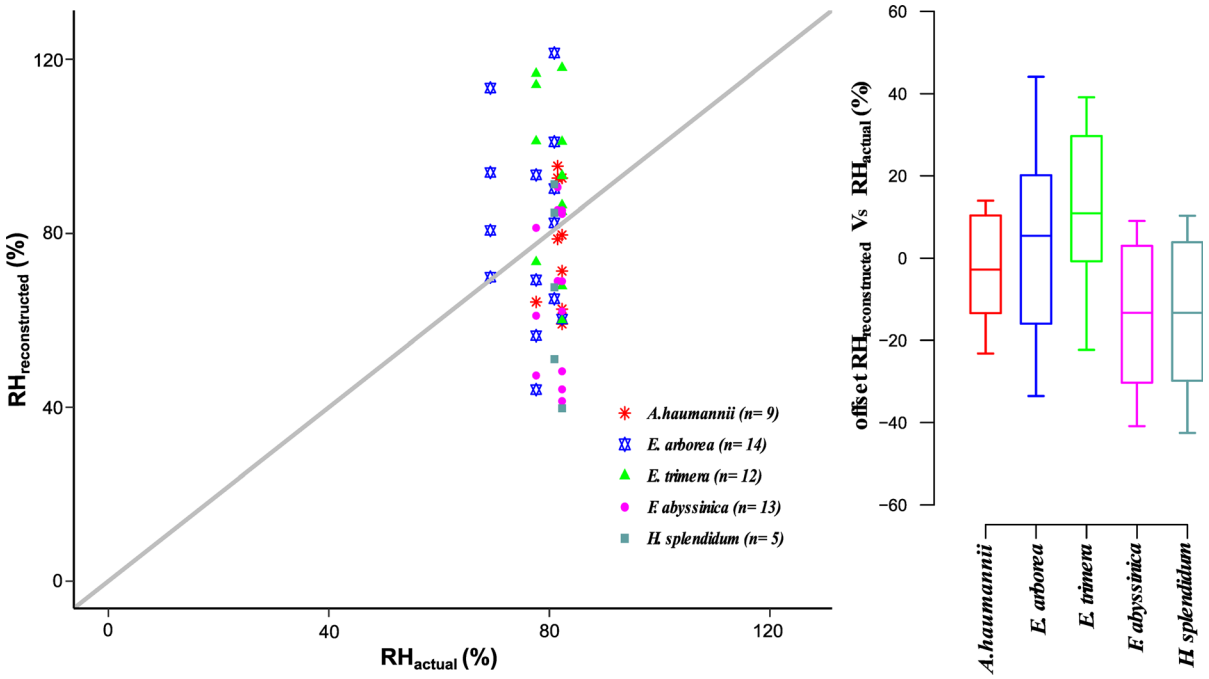

Fig. 8 The scatter plot to the left shows the correlation between reconstructed RH and actual RH. A 1:1 regression line (grey line) are provided. The box plots to the right illustrate the offset of reconstructed RH to actual RH for dominant plant species. The plots indicate the median (solid line between the boxes), interquartile range (IQR) with upper (75%) and lower (25%) quartiles

ε_{bio} values for ^{18}O and ^{2}H of + 2‰ and + 10‰ would increase the reconstructed RH by + 8% and 6%, respectively (Hepp et al. 2017).

The actual mean annual day time RH measured along the transect is 80 ± 3.4%, which is + 2 ± 18% higher than the reconstructed mean RH. The reconstructed RH is humidity normalized to leaf temperature. Usually, leaf temperature is higher than the actual ambient temperature (Gates 1980). Thus, the difference between actual and reconstructed RH might be associated with leaf–air temperature differences (Hepp et al. 2017; Zech et al. 2013b). Additionally, our approach does not consider evaporative enrichment of soil water (Zech et al. 2013b; Hepp et al. 2015; Tuthorn et al. 2015). Moreover, most leaf–derived biomarkers are biosynthesized at an early stage of leaf ontogeny (Gershenzon et al. 2000; Tipple et al. 2013) and may not reflect the mean annual isotopic composition of precipitation, but rather the isotopic composition of precipitation during the growing season.

The reconstructed RH correlates highly significant and negatively with $\delta^{18}O_{leaf\ water}$ ($r = -0.7$, $p < 0.0001$, n = 53, ESM_4 of the supplementary files) and positively with $\delta^{2}H_{leaf\ water}$ ($r = 0.6$, $p < 0.0001$, n = 53, ESM_5 of the supplementary files). This result might demonstrate that signal changes in $\delta^{18}O_{leaf\ water}$ due to RH are dissociated from signal changes in $\delta^{18}O_{prec}$. The negative correlation between the reconstructed RH and $\delta^{18}O_{leaf\ water}$, apparent in the present study, is also reported previously by Zech et al. (2013b). Thus, due to evaporation, the lower the reconstructed RH is the higher $\delta^{18}O_{leaf\ water}$. Moreover, the reconstructed RH values correlate highly significantly and positively with reconstructed $\delta^{2}H_{source\ water}$ and $\delta^{18}O_{source\ water}$ ($r = 0.9$, $p < 0.0001$, n = 53, ESM_6 and 7 of the supplementary files). A similar finding was reported by Hepp et al. (2017) applying the coupled $\delta^{2}H_{n\text{- alkane}}$ –$\delta^{18}O_{sugar}$ approach in the Mt. Kilimanjaro region.

Conclusion

The compound–specific stable hydrogen and oxygen isotopic composition of biomarkers (*n*-alkanes and sugars) analysed from leaves, O–layers, and A_h–

horizons along an altitudinal transect in the Bale Mountains were evaluated. There are no systematic $\delta^2H_{n\text{-alkane}}$ and $\delta^{18}O_{sugar}$ trends and significant differences between leaves and corresponding O–layers, and A_h–horizons, respectively. Hence, there is no evidence from our dataset for degradation and underground root input affecting $\delta^2H_{n\text{-alkane}}$ and $\delta^{18}O_{sugar}$ values of topsoils. The dominant plant species in the Bale Mountains are characterized by statistically significant species–dependent $\delta^2H_{n\text{-alkane}}$ values and, albeit not significant, also $\delta^{18}O_{sugar}$ values. Substantial species–specific apparent isotope fractionation highlights the importance of investigating apparent as well as biosynthetic isotope fractionation factor of the representative flora at a given geographical region. As a broader implication vegetation changes need to be considered when aiming at reconstructing δ^2H_{prec} from $\delta^2H_{n\text{-alkanes}}$. The coupled $\delta^2H_{n\text{-alkane}}$ –$\delta^{18}O_{sugar}$ approach allows reconstructing δ^2H and $\delta^{18}O$ of leaf water and plant source water. The latter show large scattering and on average 11.3‰ and 2.6‰ more positive δ^2H and $\delta^{18}O$ values, respectively, compared to precipitation. The reconstructed *d*-excess of leaf water enables us to reconstruct RH. The actual mean annual day time RH measured in the Bale Mountains is $+ 2 \pm 18\%$ higher than the reconstructed mean RH. The coupled $\delta^2H_{n\text{-alkane}}$ –$\delta^{18}O_{sugar}$ (paleo–) hygrometer approach as recently validated also by Hepp et al. (2020b) therefore holds great potential for deriving additional paleoclimatic information compared to single isotope approaches.

Acknowledgements The authors are indebted for the scientific collaboration and technical support obtained from Addis Ababa University, Ethiopian Biodiversity Institute, and Ethiopian Wildlife Conservation Authority. We appreciate Heike Maennicke and Marianne Benesch for laboratory assistance and measurement of compound–specific isotopes, respectively. Furthermore, we are also grateful for the assistance provided by Betelhem Mekonnen and Tobias Bromm during sample collection and sugar biomarker analyses. Mr. Bruk Lemma greatly appreciates the funding via a PhD fellowship by the Catholic Academic Exchange Services (KAAD).

Author contributions Sample collection, Formal analysis and Investigation, Writing—original draft: [BL]; Formal analysis, Writing—review and editing: [LB]; Funding acquisition, Resources, Writing—review and editing, Supervision: [BG]; Writing—review and editing, Supervision: [SK]; Writing—review and editing, Supervision: [SN]; Funding acquisition, Sample collection, Writing—review and editing, Supervision: [WZ]; Funding acquisition, Conceptualization, Methodology, Writing—review and editing, Supervision: [MZ].

Funding Open Access funding enabled and organized by Projekt DEAL. This research work was funded by the German Research Foundation within the DFG Research Unit 'The Mountain Exile Hypothesis' (DFG: ZE 844/10–1, GL 327/18–1,2, ZE 154/70–1,2). We acknowledge the financial support within the funding programme Open Access Publishing by the DFG.

Availability of data and materials Supplementary data are provided and available https://doi.org/10.5281/zenodo.4072011.

Declaration

Conflict of interest The authors have no conflicts of interest to declare that are relevant to the content of this article.

References

Allison GB, Gat JR, Leaney FW (1985) The relationship between deuterium and oxygen-18 delta values in leaf water. Chem Geol (Isotope Geoscience Section) 58:145–156

Amelung W, Cheshire MV, Guggenberger G (1996) Determination of neutral and acidic sugars in soil by capillary gas-liquid chromatography after trifluoroacetic acid hydrolysis. Soil Biol Biochem 28:1631–1639

Billi P (2015) Geomorphological landscapes of Ethiopia. Landscapes and landforms of Ethiopia. Springer, Dordrecht, pp 3–32

Bittner L, Bliedtner M, Grady D et al (2020) Revisiting afro-alpine Lake Garba Guracha in the Bale Mountains of Ethiopia: rationale, chronology, geochemistry, and paleoenvironmental implications. J Paleolimnol 64:293–314

Brittingham A, Hren MT, Hartman G (2017) Microbial alteration of the hydrogen and carbon isotopic composition of n-alkanes in sediments. Org Geochem 107:1–8

Buggle B, Zech M (2015) New frontiers in the molecular based reconstruction of Quaternary paleovegetation from loess and paleosols. Quat Int 372:180–187

Cernusak LA, Wong SC, Farquhar GD (2003) Oxygen isotope composition of phloem sap in relation to leaf water in *Ricinus communis*. Funct Plant Biol 30:1059–1070

Coffinet S, Huguet A, Pedentchouk N et al (2017) Evaluation of branched GDGTs and leaf wax n-alkane δ^2H as (paleo) environmental proxies in East Africa. Geochim Cosmochim Acta 198:182–193

Craig H (1961) Isotopic variations in meteoric waters. Science 133:1702–1703

Craig H, Gordon LI (1965) Deuterium and oxygen 18 variations in the ocean and the marine atmosphere. Laboratorio di geologia nucleare, Pisa, p 122

Dansgaard W (1964) Stable isotopes in precipitation. Tellus 16:436–468

Dongmann G, Nürnberg HW, Förstel H, Wagener K (1974) On the enrichment of $H_2{}^{18}O$ in the leaves of transpiring plants. Radiat Environ Biophys 11:41–52

Eglinton TI, Eglinton G (2008) Molecular proxies for paleoclimatology. Earth Planet Sci Lett 275:1–16

Eglinton G, Hamilton RJ (1967) Leaf epicuticular waxes. Science 156:1322–1335

Ehleringer JR, Phillips SL, Schuster WS, Sandquist DR (1991) Differential utilization of summer rains by desert plants. Oecologia 88:430–434

Ellsworth PZ, Williams DG (2007) Hydrogen isotope fractionation during water uptake by woody xerophytes. Plant Soil 291:93–107

Farquhar GD, Cernusak LA, Barnes B (2007) Heavy water fractionation during transpiration. Plant Physiol 143:11–18

Feakins SJ, Sessions AL (2010) Controls on the D/H ratios of plant leaf waxes in an arid ecosystem. Geochim Cosmochim Acta 74:2128–2141

Flanagan LB, Comstock JP, Ehleringer JR (1991) Comparison of modeled and observed environmental influences on the stable oxygen and hydrogen isotope composition of leaf water in *Phaseolus vulgaris* L. Plant Physiol 96:588

Friis I (1986) Zonation of forest vegetation on the south slope of Bale Mountains, South Ethiopia. Sinet 9:29–44

Gamarra B, Sachse D, Kahmen A (2016) Effects of leaf water evaporative ^2H-enrichment and biosynthetic fractionation on leaf wax n-alkane δ^2H values in C3 and C4 grasses. Plant, Cell Environ 39:2390–2403

Gao L, Guimond J, Thomas E, Huang Y (2015) Major trends in leaf wax abundance, δ^2H and $\delta^{13}C$ values along leaf venation in five species of C3 plants: physiological and geochemical implications. Org Geochem 78:144–152

Gat JR, Bowser C (1991) The heavy isotope enrichment of water in coupled evaporative systems. Stable isotope geochemistry: a tribute to Samuel Epstein. The Geochemical Society, St. Louis, pp 159–168

Gat JR, Yakir D, Goodfriend G et al (2007) Stable isotope composition of water in desert plants. Plant Soil 298:31–45

Gates DM (1980) Biophysical ecology. Springer-Verlag, New York, p 611

Gershenzon J, McConkey ME, Croteau RB (2000) Regulation of monoterpene accumulation in leaves of peppermint. Plant Physiol 122:205–214

Gessler A, Brandes E, Buchmann N et al (2009) Tracing carbon and oxygen isotope signals from newly assimilated sugars in the leaves to the tree-ring archive. Plant Cell Environ 32:780–795

Gessler A, Brandes E, Keitel C et al (2013) The oxygen isotope enrichment of leaf-exported assimilates–does it always reflect lamina leaf water enrichment? New Phytol 200:144–157

Gil-Romera G, Adolf C, Benito BM et al (2019) Long-term fire resilience of the Ericaceous Belt, Bale Mountains, Ethiopia. Biol Lett 15:20190357

Glaser B, Zech W (2005) Reconstruction of climate and landscape changes in a high mountain lake catchment in the Gorkha Himal, Nepal during the Late Glacial and Holocene as deduced from radiocarbon and compound-specific stable isotope analysis of terrestrial, aquatic and microbial biomarkers. Org Geochem 36:1086–1098

Griepentrog M, De Wispelaere L, Bauters M et al (2019) Influence of plant growth form, habitat and season on leaf-wax n-alkane hydrogen-isotopic signatures in equatorial East Africa. Geochim Cosmochim Acta 263:122–139

Guo N, Gao J, He Y et al (2014) Variations in leaf epicuticular n-alkanes in some *Broussonetia*, *Ficus* and *Humulus* species. Biochem Syst Ecol 54:150–156

Hedberg O (1964) Features of Afroalpine plant ecology. Uppsala: Svenska växtgeografiska Sällskapet. Acta Phytogeographica Suecica; 49. Almqvist and Wiksells, Uppsala, p 144

Helliker BR, Ehleringer JR (2002) Grass blades as tree rings: environmentally induced changes in the oxygen isotope ratio of cellulose along the length of grass blades. New Phytol 155:417–424

Hepp J, Tuthorn M, Zech R et al (2015) Reconstructing lake evaporation history and the isotopic composition of precipitation by a coupled $\delta^{18}O$–δ^2H biomarker approach. J Hydrol 529:622–631

Hepp J, Zech R, Rozanski K et al (2017) Late Quaternary relative humidity changes from Mt. Kilimanjaro, based on a coupled ^2H–^{18}O biomarker paleohygrometer approach. Quat Int 438:116–130

Hepp J, Wüthrich L, Bromm T et al (2019) How dry was the Younger Dryas? Evidence from a coupled δ^2H–$\delta^{18}O$ biomarker paleohygrometer applied to the Gemündener Maar sediments, Western Eifel, Germany. Climate Past 15:713–733

Hepp J, Mayr C, Rozanski K et al (2020a) Validation of a coupled $\delta^2H_{n\text{-alkane}}$–$\delta^{18}O_{sugar}$ paleohygrometer approach based on a climate chamber experiment. Biogeosci Discuss. https://doi.org/10.5194/bg-2020-434

Hepp J, Schäfer IK, Lanny V et al (2020b) Evaluation of bacterial glycerol dialkyl glycerol tetraether and ^2H–^{18}O biomarker proxies along a central European topsoil transect. Biogeosciences 17:741–756

Hillman JC (1986) Conservation in Bale mountains national park, Ethiopia. Oryx 20:89–94

Hillman JC (1988) The Bale Mountains National Park area, southeast Ethiopia, and its management. Mt Res Dev 8:253–258

Horita J, Wesolowski DJ (1994) Liquid-vapor fractionation of oxygen and hydrogen isotopes of water from the freezing to the critical temperature. Geochim Cosmochim Acta 58:3425–3437

Jaeschke A, Rethemeyer J, Lappé M et al (2018) Influence of land use on distribution of soil n-alkane δD and brGDGTs

along an altitudinal transect in Ethiopia: implications for (paleo) environmental studies. Org Geochem 124:77–87

Kidane Y, Stahlmann R, Beierkuhnlein C (2012) Vegetation dynamics, and land use and land cover change in the Bale Mountains, Ethiopia. Environ Monit Assess 184:7473–7489

Ladd SN, Sachs JP (2015) Influence of salinity on hydrogen isotope fractionation in Rhizophora mangroves from Micronesia. Geochim Cosmochim Acta 168:206–221

Lemma B, Grehl C, Zech M et al (2019a) Phenolic compounds as unambiguous chemical markers for the identification of keystone plant species in the bale mountains, Ethiopia. Plants 8:228

Lemma B, Mekonnen B, Glaser B et al (2019b) Chemotaxonomic patterns of vegetation and soils along altitudinal transects of the Bale Mountains, Ethiopia, and implications for paleovegetation reconstructions–part II: lignin-derived phenols and leaf-wax-derived n-alkanes. E&G Quat Sci J 68:189–200

Lemma B, Kebede Gurmessa S, Nemomissa S et al (2020) Spatial and temporal ^{2}H and ^{18}O isotope variation of contemporary precipitation in the Bale Mountains, Ethiopia. Isot Environ Health Stud 56:122–135

Liu W, Yang H (2008) Multiple controls for the variability of hydrogen isotopic compositions in higher plant n-alkanes from modern ecosystems. Glob Change Biol 14:2166–2177

McInerney FA, Helliker BR, Freeman KH (2011) Hydrogen isotope ratios of leaf wax n-alkanes in grasses are insensitive to transpiration. Geochim Cosmochim Acta 75:541–554

Mekonnen B, Zech W, Glaser B et al (2019) Chemotaxonomic patterns of vegetation and soils along altitudinal transects of the Bale Mountains, Ethiopia, and implications for paleovegetation reconstructions–part 1: stable isotopes and sugar biomarkers. E&G Quat Sci J 68:177–188

Merlivat L (1978) Molecular diffusivities of $H_2{}^{16}O$, $HD^{16}O$, and $H_2{}^{18}O$ in gases. J Chem Phys 69:2864–2871

Miehe S, Miehe G (1994) Ericaceous forests and heathlands in the Bale Mountains of South Ethiopia. Ecology and man's impact. Warnke, Hamburg, p 206

Osmaston HA, Mitchell WA, Osmaston JN (2005) Quaternary glaciation of the Bale Mountains, Ethiopia. J Quat Sci 20:593–606

Ossendorf G, Groos AR, Bromm T et al (2019) Middle Stone Age foragers resided in high elevations of the glaciated Bale Mountains, Ethiopia. Science 365:583–587

Peterse F, van Der Meer MTJ, Schouten S et al (2009) Assessment of soil n-alkane δD and branched tetraether membrane lipid distributions as tools for paleoelevation reconstruction. Biogeosciences 6:2799–2807

Roden JS, Ehleringer JR (1999) Observations of hydrogen and oxygen isotopes in leaf water confirm the Craig-Gordon model under wide-ranging environmental conditions. Plant Physiol 120:1165–1173

Rozanski K, Araguás-Araguás L, Gonfiantini R (1993) Isotopic patterns in modern global precipitation. Climate change in continental isotopic records. American Geophysical Union, Washington, D.C., pp 1–36

Sachse D, Billault I, Bowen GJ et al (2012) Molecular paleohydrology: interpreting the hydrogen-isotopic composition of lipid biomarkers from photosynthesizing organisms. Annu Rev Earth Planet Sci 40:221–249

Schmidt H-L, Werner RA, Roßmann A (2001) ^{18}O pattern and biosynthesis of natural plant products. Phytochemistry 58:9–32

Sessions AL, Burgoyne TW, Schimmelmann A, Hayes JM (1999) Fractionation of hydrogen isotopes in lipid biosynthesis. Org Geochem 30:1193–1200

Sternberg da LSL (1989) Oxygen and hydrogen isotope ratios in plant cellulose: mechanisms and applications. Stable isotopes in ecological research. Springer, New York, pp 124–141

Strobel P, Haberzettl T, Bliedtner M et al (2020) The potential of $\delta^{2}H_{n\text{-alkanes}}$ and $\delta^{18}O_{sugar}$ for paleoclimate reconstruction—a regional calibration study for South Africa. Sci Total Environ 716:137045

Tiercelin J-J, Gibert E, Umer M et al (2008) High-resolution sedimentary record of the last deglaciation from a high-altitude lake in Ethiopia. Quat Sci Rev 27:449–467

Tipple BJ, Berke MA, Doman CE et al (2013) Leaf-wax n-alkanes record the plant–water environment at leaf flush. Proc Natl Acad Sci USA 110:2659–2664

Tu TTN, Egasse C, Zeller B et al (2011) Early degradation of plant alkanes in soils: a litterbag experiment using 13C-labelled leaves. Soil Biol Biochem 43:2222–2228

Tuthorn M, Zech M, Ruppenthal M et al (2014) Oxygen isotope ratios ($^{18}O/^{16}O$) of hemicellulose-derived sugar biomarkers in plants, soils and sediments as paleoclimate proxy II: insight from a climate transect study. Geochim Cosmochim Acta 126:624–634

Tuthorn M, Zech R, Ruppenthal M et al (2015) Coupling $\delta^{2}H$ and $\delta^{18}O$ biomarker results yields information on relative humidity and isotopic composition of precipitation—a climate transect validation study. Biogeosciences 12:3913–3924

Umer M, Kebede S, Osmaston H (2004) Quaternary glacial activity on the Ethiopian Mountains. Developments in Quaternary Sciences. Elsevier, Amsterdam, pp 171–174

Umer M, Lamb HF, Bonnefille R et al (2007) Late pleistocene and Holocene vegetation history of the bale mountains, Ethiopia. Quat Sci Rev 26:2229–2246

Voelker SL, Brooks JR, Meinzer FC et al (2014) Reconstructing relative humidity from plant $\delta^{18}O$ and δD as deuterium deviations from the global meteoric water line. Ecol Appl 24:960–975

Walker CD, Brunel J-P (1990) Examining evapotranspiration in a semi-arid region using stable isotopes of hydrogen and oxygen. J Hydrol 118:55–75

White JW, Cook ER, Lawrence JR (1985) The DH ratios of sap in trees: Implications for water sources and tree ring DH ratios. Geochim Cosmochim Acta 49:237–246

Woldu Z, Feoli E, Nigatu L (1989) Partitioning an elevation gradient of vegetation from southeastern Ethiopia by probabilistic methods. Numerical syntaxonomy. Springer, Dordrecht, pp 189–198

Yimer F, Ledin S, Abdelkadir A (2006) Soil organic carbon and total nitrogen stocks as affected by topographic aspect and vegetation in the Bale Mountains, Ethiopia. Geoderma 135:335–344

Zech M, Glaser B (2008) Improved compound-specific $\delta^{13}C$ analysis of n-alkanes for application in

palaeoenvironmental studies. Rapid Commun Mass Spectrom 22:135–142

Zech M, Glaser B (2009) Compound-specific $\delta^{18}O$ analyses of neutral sugars in soils using gas chromatography–pyrolysis–isotope ratio mass spectrometry: problems, possible solutions and a first application. Rapid Commun Mass Spectrom 23:3522–3532

Zech M, Buggle B, Leiber K et al (2009) Reconstructing Quaternary vegetation history in the Carpathian Basin, SE Europe, using n-alkane biomarkers as molecular fossils: problems and possible solutions, potential and limitations. E&G Quat Sci J 58:148–155

Zech M, Pedentchouk N, Buggle B et al (2011) Effect of leaf litter degradation and seasonality on D/H isotope ratios of n-alkane biomarkers. Geochim Cosmochim Acta 75:4917–4928

Zech M, Rass S, Buggle B et al (2012a) Reconstruction of the late Quaternary paleoenvironments of the Nussloch loess paleosol sequence, Germany, using n-alkane biomarkers. Quat Res 78:226–235

Zech M, Werner RA, Juchelka D et al (2012b) Absence of oxygen isotope fractionation/exchange of (hemi-) cellulose derived sugars during litter decomposition. Org Geochem 42:1470–1475

Zech M, Rass S, Buggle B et al (2013a) Reconstruction of the late Quaternary paleoenvironments of the Nussloch loess paleosol–response to comments by G. Wiesenberg and M. Gocke. Quat Res 79:306–307

Zech M, Tuthorn M, Detsch F et al (2013b) A 220 ka terrestrial $\delta^{18}O$ and deuterium excess biomarker record from an eolian permafrost paleosol sequence, NE-Siberia. Chem Geol 360:220–230

Zech M, Mayr C, Tuthorn M et al (2014a) Oxygen isotope ratios ($^{18}O/^{16}O$) of hemicellulose-derived sugar biomarkers in plants, soils and sediments as paleoclimate proxy I: insight from a climate chamber experiment. Geochim Cosmochim Acta 126:614–623

Zech M, Tuthorn M, Zech R et al (2014b) A 16-ka $\delta^{18}O$ record of lacustrine sugar biomarkers from the High Himalaya reflects Indian Summer Monsoon variability. J Paleolimnol 51:241–251

Zech M, Zech R, Rozanski K et al (2015) Do n-alkane biomarkers in soils/sediments reflect the $\delta^{2}H$ isotopic composition of precipitation? A case study from Mt. Kilimanjaro and implications for paleoaltimetry and paleoclimate research. Isot Environ Health Stud 51:508–524